Anal. Chem. **2009,** *81,* 6687–6694

Visualizing the Size, Shape, Morphology, and Localized Surface Plasmon Resonance of Individual Gold Nanoshells by Near-Infrared Multispectral Imaging Microscopy

Irena Mejac,[†] William W. Bryan,[‡] T. Randall Lee,[‡] and Chieu D. Tran*,[†]

Department of Chemistry, Marquette University, P.O. Box 1881, Milwaukee, Wisconsin 53201, and Department of Chemistry, University of Houston, 4800 Calhoun Road, Houston, Texas 77204

We have successfully utilized the newly developed near-infrared multispectral imaging (NIR-MSI) microscope to observe and measure *directly* the localized surface plasmon absorption (LSPR) of *individual* gold nanoshells. The NIR-MSI is suited for this task because it can simultaneously record spectral and spatial information of a sample with high sensitivity (single pixel resolution) and high spatial resolution (~0.9 μm/pixel). Importantly, the LSPR of individual nanoshells measured by the NIR-MSI microscope agrees well with the spectra calculated theoretically using Mie scattering for the nanoshells (i.e., nanoshells with silica cores ~800 nm in diameter and gold shell thicknesses of ~35 nm). Additionally, the NIR-MSI microscope enables measurement of LSPR at different positions within a single nanoshell. LSPR spectra were found to be distinct at various positions within a single nanoshell. Since LSPR spectra are known to depend on the shape and morphology of the nanoshells, these results seem to suggest that the individual nanoshells are not smooth and well-defined, but are rather rough and inhomogeneous. The LSPR spectra of single nanoshells in several different solvents were also examined using NIR-MSI and were found to depend on the dielectric constant of the medium. However, the relationship was discovered to be more complex than simply following the Drude equation. Specifically, when $(\lambda_{max}/\mathrm{fwhm})^2$ values of LSPR for single gold nanoshells were plotted as a function of $2n^2$ (or 2ϵ) for nanoshells in six different solvents, a linear relationship was found for only three solvents: D_2O, acetonitrile-d_3, and ethyl acetate. Acetone-d_6 showed a slight deviation, whereas formamide and pyridine-d_5 exhibited distinctly different correlations.

The optical properties of noble metal nanoparticles are the subject of intense interest because of their extensive use as functional materials in applications such as optical devices, energy transport, near-field scanning optical microscopy, surface-enhanced spectroscopies, and chemical and biochemical sensors.[1−3] Noble metal nanoparticles exhibit a strong absorption band that arises when the incident photon frequency is resonant with the collective oscillation of the electrons and is known as the localized surface plasmon resonance (LSPR).[1−3] The properties of the LSPR are controlled by the dielectric function of the constituent metal and the embedding medium, and also by the shape of the nanostructure.[1−3] For nanoshells, the shell/core ratio is largely responsible for the plasmon resonance frequency supported by this geometry.[4−6]

A number of groups have reported the absorption spectra of nanoparticles and nanoshells prepared in water and in organic solvents. However, comparison of the spectra is not easy because of differences in particle shape, size, distribution, and stability. Specifically, key structural parameters such as the aspect ratio, cap-end shape, and volume of the particles are frequently polydisperse, leading to strong inhomogeneities in the optical response. This lack of monodispersity makes it difficult to compare not only data obtained from different experiments but also data derived from experiment and computation. As a consequence, it is difficult to analyze quantitatively the efficiency of the nanoshells in applications such as those based on field-enhancement effects.

To overcome the inhomogeneous broadening inherent in ensemble measurements, single-particle spectra are desired. Such challenges have prompted considerable efforts in the past few years to develop a technique that can measure the plasmon modes of single nanoparticles. Limited success has been made, including the use of such techniques as scanning near-field optical microscopy (SNOM), dark field illumination (DF), high resolution electron energy loss spectroscopy, and spatial modulation spec-

* To whom correspondence should be addressed. E-mail: chieu.tran@marquette.edu.
[†] Marquette University.
[‡] University of Houston.

(1) Willets, K. A.; Van Duyne, R. P. *Annu. Rev. Phys. Chem.* **2007**, *58*, 267–297.
(2) Skrabalak, S. E.; Chen, J.; Sun, Y.; Lu, X.; Au, L.; Cobley, C. M.; Xia, Y. *Acc. Chem. Res.* **2008**, *41*, 1587–1595.
(3) Sun, Y.; Xia, Y. *Anal. Chem.* **2002**, *74*, 5297–5305.
(4) Westcott, S. L.; Oldenburg, S. J.; Lee, T. R.; Halas, N. J. *Langmuir* **1998**, *14*, 5396–5401.
(5) Westcott, S. L.; Oldenburg, S. J.; Lee, T. R.; Halas, N. J. *Chem. Phys. Lett.* **1999**, *300*, 651–655.
(6) Pham, T.; Jackson, J. B.; Halas, N. J.; Lee, T. R. *Langmuir* **2002**, *18*, 4915–4920.
(7) Klar, T.; Perner, M.; Grosse, S.; von Plessen, G.; Spirkl, W.; Feldman, J. *Phys. Rev. Lett.* **1998**, *80*, 4249–4252.
(8) Sonnichsen, C.; Franzl, T.; Wilk, T.; von Plessen, G.; Feldman, J.; Wilson, O.; Mulvaney, P. *Phys. Rev.* **2002**, *88*, 077402.

10.1021/ac9007495 CCC: $40.75
Published on Web 07/20/2009

troscopy to measure the absorption or scattering spectrum of a single nanoparticle.[7−10] However, apart from the serious technical challenges involved in these experiments, some techniques (e.g., SNOM and DF techniques) are limited in their ability to resolve the mode structure of the plasmon (e.g., of a metal nanorod or nanowire) spatially.[7,8] The near-infrared (NIR) multispectral imaging microscope described herein offers a simple solution to this problem.

A multispectral imaging spectrometer is an instrument that can simultaneously record spectral and spatial information about a sample.[11] Unlike conventional imaging techniques, which rely on recording a single image using either single or multiwavelength light for illumination, the multispectral imaging technique records a series of several thousand images, each image at a specific wavelength. That is, it measures absorption spectra of a sample not at a single position, as is the case for a conventional spectrophotometer, but simultaneously at many different positions within a sample (by using a focal plane array detector rather than a single channel detector).[11] Chemical composition and structure at different positions within a sample can be elucidated from such images.[11] We have recently developed a novel near-infrared (NIR) multispectral imaging microscope that employs an acousto-optic tunable filter (AOTF) for rapid spectral tuning and a microscope for higher spatial resolution.[12−20] The high sensitivity (single pixel resolution), fast temporal (milliseconds) and high spatial resolution (~μm) of this imaging microscope, make it possible for us to use this multispectral imaging microscope for studies and measurements that, to date, have not been possible using existing techniques. These include photoinduced changes of a single unit micrometer-size cell in temperature-sensitive liquid crystals as a function of time and wavelength,[16] and the determination of molecular state and distribution of fullerenes entrapped in sol−gel samples.[20]

The information presented in the present manuscript is indeed provocative and demonstrates that discrete gold nanoshells ~1 μm in diameter can be individually observed, and their LSPR spectra can be measured using multispectral imaging microscopy. Such considerations prompted us to initiate this study, which aims to (1) develop novel synthetic methods to prepare novel gold nanoshells about ~1 μm in diameter, (2) explore the use of the multispectral imaging microscope as a sensitive and effective method to observe and characterize the gold nanoshells by measuring LSPR spectra at several different positions within a single nanoshell, and also of many different single nanoshells of the same sample, and (3) determine the effect of dielectric function of the medium by measuring LSPR spectra of single nanoshells in different solvents, including D_2O, acetonitrile-d_3, acetone-d_6, ethyl acetate, pyridine-d_5, and formamide. The results of our initial investigation are reported herein.

EXPERIMENTAL SECTION

Materials. All reagents were purchased and used as received from the indicated suppliers: sodium hydroxide, ammonium hydroxide (30% NH_3), formaldehyde, nitric acid, hydrochloric acid (all from EM Science), tetrakis(hydroxymethyl)phosphonium chloride (THPC, 80% in water), potassium carbonate, 3-aminopropyltrimethoxysilane (APTMS; all from Aldrich), ethanol (Pharmco-Aaper), 0.80 μm silica microspheres (Bangs Laboratories), D_2O, acetone-d_6, acetonitrile-d_3, and pyridine-d_5 (all from Cambridge Isotope Laboratories), and hydrogen tetrachloroaurate(III) hydrate (Strem). Water was purified to a resistance of 18 MΩ (Milli-Q Reagent Water System; Millipore Corporation) and filtered through a 0.2 μm membrane filter to remove any impurities. All glassware and equipment were cleaned in an aqua regia solution (3:1, HCl/HNO_3) and then soaked in a saturated KOH/isopropyl alcohol base bath.

Preparation of Amine-Functionalized Silica Microspheres and Attachment of Gold Seeds. Amine-functionalized silica microspheres were prepared using an established procedure.[4−6,21,22] Briefly, silica microspheres (0.1 g) were added to an ethanolic solution of ammonium hydroxide containing aminopropyltrimethoxysilane (APTMS; 2.0 mL). The solution was stirred for 2 h and then refluxed for 1 h. The amine-functionalized silica microspheres were centrifuged at 2000 rpm for 1 h (RC-3B Refrigerated Centrifuge from Sorvall Instruments) and redispersed twice in 50 mL of ethanol.

Small gold "seed" particles having diameters of 2−3 nm were prepared using an established procedure,[6,21,22] which is briefly described here. To a 100 mL aqueous solution of sodium hydroxide (1.0 mL, 0.024 g, 0.6 mmol) and THPC (24 μL of THPC in 2 mL of water) was quickly added an aliquot (4 mL) of 1 wt % aqueous $HAuCl_4 \cdot H_2O$. The mixture was stirred for 30 min and then aged for 3 days in the refrigerator. An aliquot of amine-functionalized silica microspheres (0.5 mL) was then added to the aged colloidal gold solution, and the mixture was allowed to react overnight to afford THPC gold-seeded silica microspheres.[6,21−23]

Growth of Gold Nanoshells.[6,22,23] For the growth of gold nanoshells on the THPC gold-seeded silica microspheres, a basic solution of gold salt (4 mL), which was prepared by dissolving potassium carbonate (0.05 g) in 200 mL of water and adding 4 mL of a 1 wt % $HAuCl_4 \cdot H_2O$ solution, was added to a 25 mL beaker and stirred. An aliquot of purified gold-seeded silica microspheres (0.5 mL) was then added. After stirring the mixture for 5 min, 0.05 mL of formaldehyde was added as a reducing agent to form the gold shell.

As described in the preceding paragraph, the gold nanoshells were prepared as an aqueous suspension (i.e., dispersed in H_2O). To avoid complications from strong O−H absorbances, the water was exchanged to D_2O. This exchange was accomplished by centrifuging 1 mL of the H_2O solution of nanoshells at 2000

(9) N'Gom, M.; Ringnalda, J.; Mansfield, J. F.; Agarwal, A.; Kotov, N.; Zaluzec, N. J.; Norris, T. B. *Nano Lett.* **2008**, *8*, 3200–3204.
(10) Muskens, O. L.; Bachelier, G.; Fatti, N. D.; Vallee, F.; Brioude, A.; Jiang, X.; Pileni, M. P. *J. Phys. Chem. C* **2008**, *112*, 8917–8921.
(11) Morris, M. D. *Microscopic and Spectroscopic Imaging of the Chemical State*; Marcel Dekker: New York, 1993.
(12) Tran, C. D.; Cui, Y.; Smirnov, S. *Anal. Chem.* **1998**, *70*, 4701–4708.
(13) Fischer, M.; Tran, C. D. *Anal. Chem.* **1999**, *71*, 953–959.
(14) Fischer, M.; Tran, C. D. *Anal. Chem.* **1999**, *71*, 2255–2261.
(15) Tran, C. D. *J. Near-Infrared Spectrosc.* **2000**, *8*, 87–99.
(16) Khait, O.; Smirnov, S.; Tran, C. D. *Anal. Chem.* **2001**, *73*, 732–739.
(17) Tran, C. D. *Fresenius J. Anal. Chem.* **2001**, *369*, 313–319.
(18) Tran, C. D. *Appl. Spectrosc. Rev.* **2003**, *38*, 133–153.
(19) Tran, C. D. *Anal. Lett.* **2005**, *38*, 735–752.
(20) Tran, C. D.; Grishko, V. I.; Challa, S. *J. Phys. Chem. B* **2008**, *112*, 14548–14559.
(21) Kim, J.-H.; Chung, H.-W.; Lee, T. R. *Chem. Mater.* **2006**, *18*, 4115–4120.
(22) Kim, J.-H.; Bryan, W. W.; Lee, T. R. *Langmuir* **2008**, *24*, 11147–11152.
(23) Kim, J.-H.; Lee, T. R. *J. Biomed. Pharm. Eng.* **2008**, *2*, 29–35.

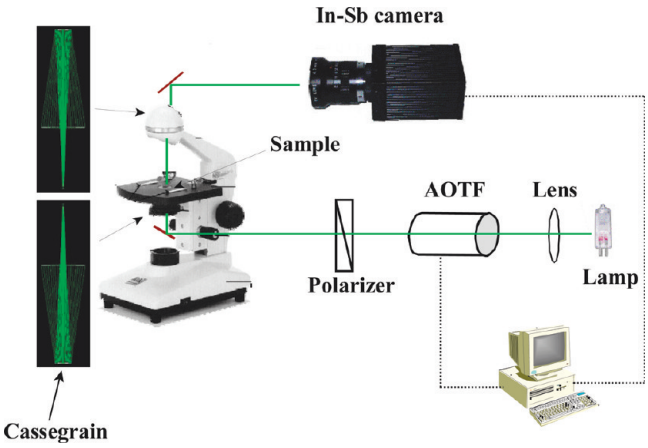

Figure 1. Schematic diagram of the near-infrared (NIR) multispectral imaging microscope.

rpm for 5 min at 22 °C. The supernatant was removed, and 1 mL of D_2O was then added. After centrifuging the sample again at 2000 rpm for 5 min, the supernatant was removed, and the nanoshells were then redispersed in 1 mL of D_2O. An analogous procedure was used to exchange H_2O to acetonitrile-d_3, acetone-d_6, ethyl acetate, pyridine-d_5, and formamide. Prior to each measurement, the sample was briefly sonicated in a water bath for 10−15 s.

Instrumentation. The acousto-optic tunable filter (AOTF) based NIR multispectral imaging microscope (Figure 1) used in this work is similar to those used in previous studies,[12−19] except for the replacement of the focusing microscopic lenses in the microscope with a pair of 0.58 N.A. 15X reflecting Cassegrains to avoid possible aberrations in the NIR region. Images recorded by the NIR camera were grabbed and transferred to a PC by a frame grabber. A software written in C++ language was used to control the imaging microscope as well as to facilitate the frame grabbing, saving and processing images. Three-dimensional (3-D) images were calculated from recorded images by use of the image processing program (National Institutes of Health, ImageJ program).

The size and morphology of the nanoshells were additionally characterized using a LEO scanning electron microscope (SEM). In these analyses, an accelerating voltage of 15 kV was used. The nanoshells were deposited from solution directly onto a silicon wafer and imaged without any additional preparation.

RESULTS AND DISCUSSION

Our initial structural characterization of the gold nanoshells consisted of imaging by SEM. Figures 2A and 2B show detailed images of the silica cores, which appear as smooth, monodisperse spheres with diameters of ∼0.80 μm. Similarly, Figures 2C and 2D show SEM images of THPC gold-seeded silica cores, which are indistinguishable in size and bulk morphology when compared to the undecorated silica core microspheres. Further, Figures 2E and 2F show SEM images of gold nanoshells, demonstrating that these composite particles are also monodisperse spheres. The thickness of the gold shells as determined by difference (see Figure 2G) was consistently ∼35 nm, giving an average diameter for the composite nanoshell particle of ∼0.87 μm. Finally, Figure 2H provides images of the batch of nanoshells used for NIR multispectral imaging (vide infra).

Two-dimensional (2-D) images of the gold nanoshell particles in D_2O and in ethyl acetate are shown in Figures 3A and 3B, respectively. Individual gold particles can be resolved in the images. As illustrated, nanoshells exist in solution in discrete form as well as in aggregated clusters. Similar images were also found for other solvents (e.g., acetone-d_6; Figure 5A). Selected sections of the 2-D images in Figures 4A (of nanoshells in ethyl acetate) and 5A (of nanoshells in acetone-d_6), indicated by the square in Figure 4A and the rectangle in Figure 5A, were then taken to calculate corresponding 3-D plots of the absorbance of the particles at 1680 nm as function of particle dimension (i.e., x and y axes with unit of pixel) (using NIH ImageJ imaging processing program). The type (discrete vs clusters) and numbers of the particles can be distinguished in the 3-D images (see Figures 4B and 5B).

On the basis of the methods described in our previous studies[12] and by using a gold U.S. Air Force resolution target as a standard, the spatial resolution of this NIR multispectral imaging instrument was determined to be 0.93 ± 0.03 μm/pixel. The average diameter of each discrete particle calculated from this relationship was found to be 1.1 ± 0.2 μm. The fact that this value is in good agreement with the value found by SEM (∼0.87 μm) lends further credence to the NIR multispectral imaging instrument. It is noteworthy that, in contrast to imaging by SEM, the NIR multispectral imaging technique can be used to observe gold nanoshells *directly in solution*. Importantly, it was found that, within experimental uncertainty, the diameter of the discrete nanoshells was found to be the same in all six solvents used in this study (i.e., D_2O, acetone-d_6, acetonitrile-d_3, ethyl acetate, pyridine-d_5, and formamide).

The three spectra shown in Figure 6A are plasmon resonance spectra recorded at three different positions within a single gold nanoshell in D_2O (i.e., these spectra were not theoretically predicted but rather were calculated from data (of recorded images) of a single pixel at three different positions within the same gold nanoshell). It is of particular interest to observe that plasmon bands at different positions within the same nanoshell are distinctly different, not only with regard to shape (i.e., spectral bandwidth), but also with regard to λ_{max}. Since the localized surface plasmon resonance (LSPR) is known to depend on the shape and morphology of the surface,[1−10] the fact that distinct plasmon bands are observed at various positions within the same nanoshell indicates that the morphology of the nanoshell surface is rough and inhomogeneous. Because nanoshell particles are in solution, they are known to undergo Brownian motion.[24−26] However, because the NIR-MSI microscope used in this study can rapidly record images of a sample (e.g., it took only 560 ms to record image shown in Figure 5A) and also because the size of the nanoshell is rather large (1.1 μm diameter), as predicted by literature,[24−26] we did not experimentally observe any Brownian motion effect on images and data reported here.

It is noteworthy to add that the observed inhomogeneities of the nanoshell surface are on the order of nanometers, which are smaller than the scale used for the SEM images; the variations

(24) Kihm, K. D.; Banerjee, A.; Choi, C. K.; Takagi, T. *Exp. Fluids* **2004**, *37*, 811–814.
(25) Tuteja, A.; Mackay, M. E.; Narayanan, S.; Asokan, S.; Wong, M. S. *Nano Lett.* **2007**, *7*, 1276–1281.
(26) Liu, J.; Cao, D.; Zhang, L. *J. Phys. Chem. C* **2008**, *112*, 6653–6661.

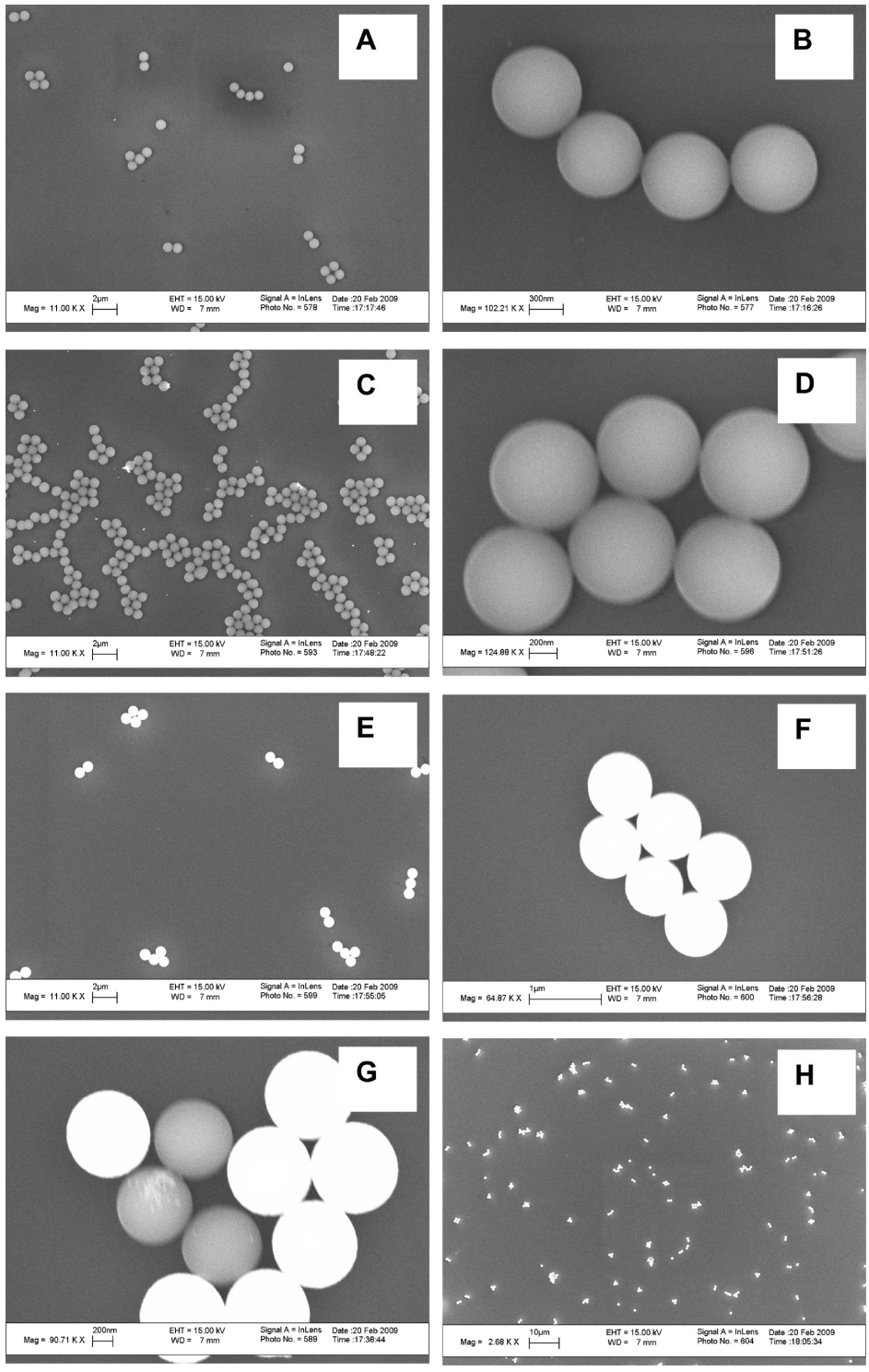

Figure 2. Scanning electron microscope (SEM) images of (A,B) silica cores, (C,D) gold seeded silica cores, (E,F) complete gold nanoshells, (G) coated and uncoated gold nanoshells, and (H) analyzed gold nanoshells.

in surface morphology were not resolved in the SEM images. An investigation that includes a side-by-side comparison of NIR multispectral imaging with transmission electron microscopy (TEM) imaging of the surface morphology of gold nanoshells will be the subject of a future report.

Because the size of the nanoshells (~1.1 μm) is comparable to the spatial resolution of the NIR imaging instrument (0.93 μm), if single-pixel data are collected from the edge of a nanoshell rather than the center, the measurement will include not only the absorbance of the nanoshell but also that of the solvent (note that absorbance by the solvent will be zero since the spectrum of the solvent will be background-subtracted). Consequently, the calculated absorbance spectrum will be an average of all of the data, with diminished peak intensities when compared to data collected from the center of a nanoshell. However, we would anticipate no changes in the position or shape of the λ_{max} bands in the absorbance spectra. This prediction is verified in Figure 6B, which shows three spectra calculated from one single position

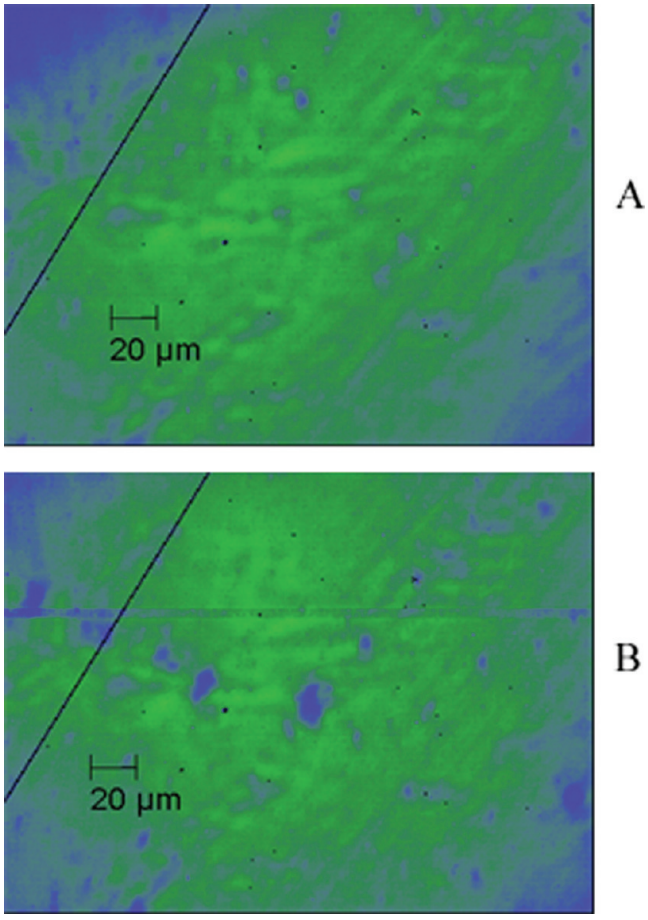

Figure 3. 2-D images at 1680 nm of gold nanoshells in D_2O solution (A) and ethyl acetate solution (B). Nanoshell particles are in blue, green is background and the black line in the upper left-hand corner is a marking of the NIR camera.

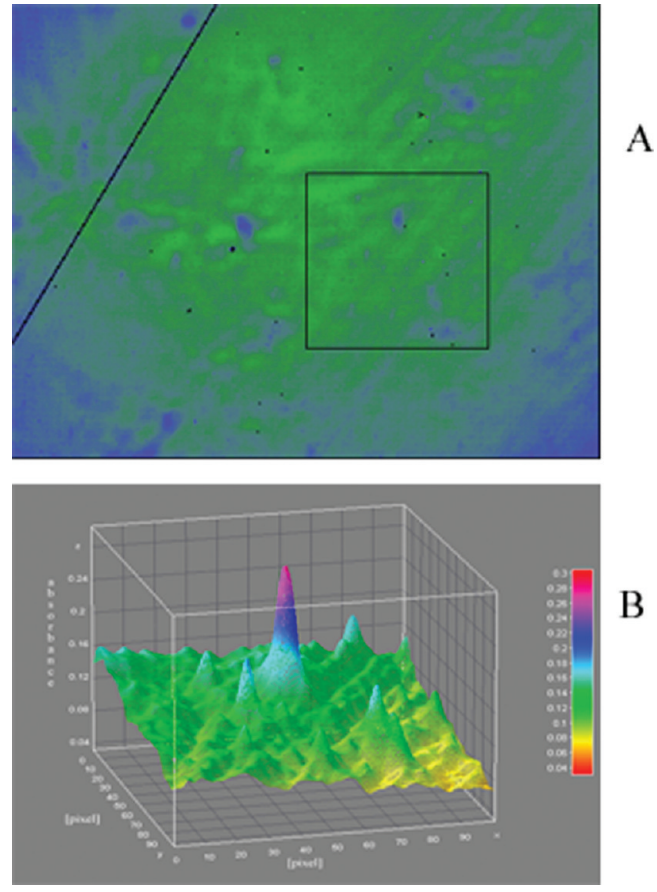

Figure 4. (A) 2-D image of absorption at 1680 nm of gold nanoshells in ethyl acetate solution; and (B) corresponding 3-D absorption image of the drawn rectangular section in (A). Units for *x*, *y*, and *z* axes are pixel, pixel, and absorbance at 1680 nm, respectively (one pixel corresponds to 0.93 μm).

within a gold nanoshell in D_2O. Again these spectra were not calculated theoretically, but rather were calculated using data (of recorded images) of a single pixel (black) and the average of a square of 3×3 pixels (green) and an average of a square of 5×5 pixels (pink). Since only one spectrum was obtained for each case (single pixel, square of 3×3 or 5×5), they cannot be correctly classified as "averaged spectra". For example, while the spectrum obtained from a square of 3×3- pixel can be considered as an averaged spectrum of 9 spectra calculated from data of a single pixel *not at the same single position but at 9 different positions within a square of 3 × 3 pixel*. As illustrated, the three spectra have the same shape and λ_{max}. The only difference among them is their intensity. The fact that spectra taken from different positions (center vs edges) of a single Au nanoshell (Figure 6A) exhibit not only different intensities but also shifts in λ_{max} and changes in bandwidth (Figure 6A) is consistent with variations in morphology across the surface of the nanoshell.

Interestingly, the value of λ_{max} shifts and the width of the LSPR band narrows when a single gold nanoshell dispersed in D_2O is transferred to acetonitrile-d_3 (see Figure 6A vs Figure 7B). Importantly, the dependency of the LSPR on the morphology of the particle was also observed in acetonitrile-d_3; namely, the spectra at three different positions within a single particle are different (Figure 7B). Furthermore, the changes in λ_{max} and spectral bandwidth of the LSPR are not specific to D_2O and acetonitrile-d_3, but are general, as they were observed for other solvents as well, including ethyl acetate (Figure 7C), pyridine-d_5 (Figure 7D), acetone-d_6 (Figure 7E), and formamide (Figure 7F). In fact, in formamide, the bandwidths of the LSPR bands became so broad that they are about three to four times broader than those in ethyl acetate. For ease of comparison, the LSPR spectra of a single gold nanoshell in the six different solvents are plotted together in Figure 8.

As illustrated in Figures 6−8, the absorbance maximum for the gold nanoshells appears roughly at 1700 nm. This value is consistent with that calculated theoretically using Mie scattering for nanoshells having silica cores ~800 nm in diameter and gold shell thicknesses of ~35 nm.[27,28] Furthermore, to our knowledge, the experimental results presented here offer the first direct measurement of the LSPR of single gold nanoshells *in solution*. This type of measurement is not possible using conventional NIR spectrophotometers because in spectrophotometric measurements, the signal from the entire solution of many particles is detected as an averaged signal by the single-channel detector. We were able to perform such measurements because our NIR multispectral imaging microscope enables us to focus on and

(27) Mie, G. *Ann. Phys.* **1908**, *25*, 377–445.
(28) Aden, A. L.; Kerker, M. *J. Appl. Phys.* **1951**, *22*, 1242–1246.

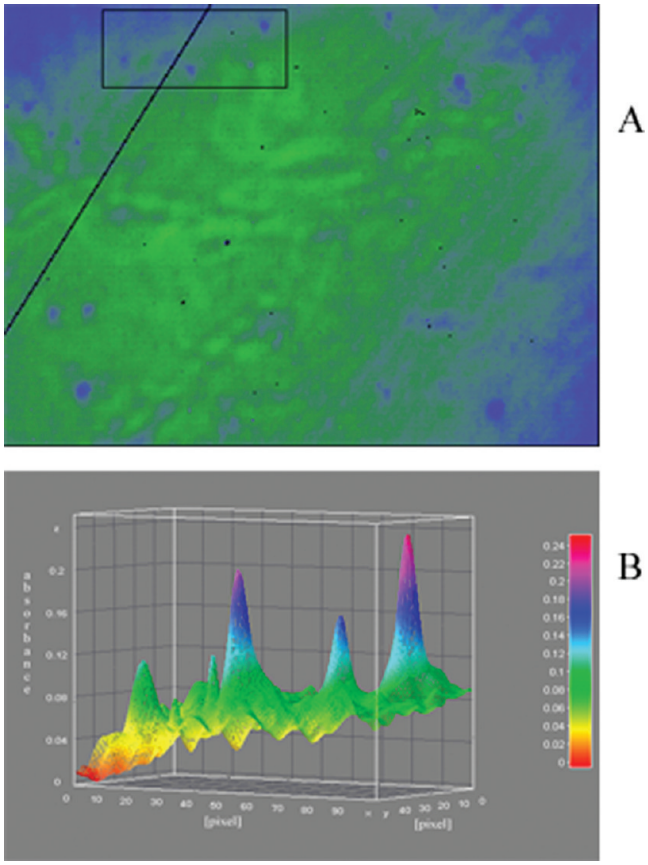

Figure 5. (A) 2-D image of absorption a t 1680 nm of gold nanoshells in acetone-d_6 solution; and (B) corresponding 3-D absorption image of the drawn square section in (A). Units for *x*, *y*, and *z* axes are pixel, pixel, and absorbance at 1680 nm, respectively (one pixel corresponds to 0.93 μm).

observe directly the NIR absorbance of a single individual nanoshell rather than the collective absorbance of multiple nanoshells in solution.

It has been theoretically predicted and experimentally verified that for relatively small gold nanoparticles and nanoshells, the variation of the maxima of the LSPR with the refractive index of the solvent can be treated within the framework of the Drude model.[1,29,30] Specifically, the surface plasmon peak position, λ, is related to the refractive index of the surrounding medium (nm) by the relation

$$\lambda^2 = \lambda_p^2(\epsilon^\infty + 2\epsilon_m) \quad (1)$$

where λ_p is the bulk metal plasmon wavelength, ϵ^∞ is the high frequency dielectric constant due to interband and core transitions, and ϵ_m ($= n^2$) is the optical dielectric function of the medium. According to this equation, a plot of λ^2 against $2\epsilon_m$ (or $2n^2$) should yield a straight line. Notably, we/others have previously observed this correlation for nanoparticles and nanoshells that exhibit narrow LSPR bands.[1−10] However, it would be difficult to apply this equation without any modification to particles that exhibit relatively broad plasmon resonance bands,

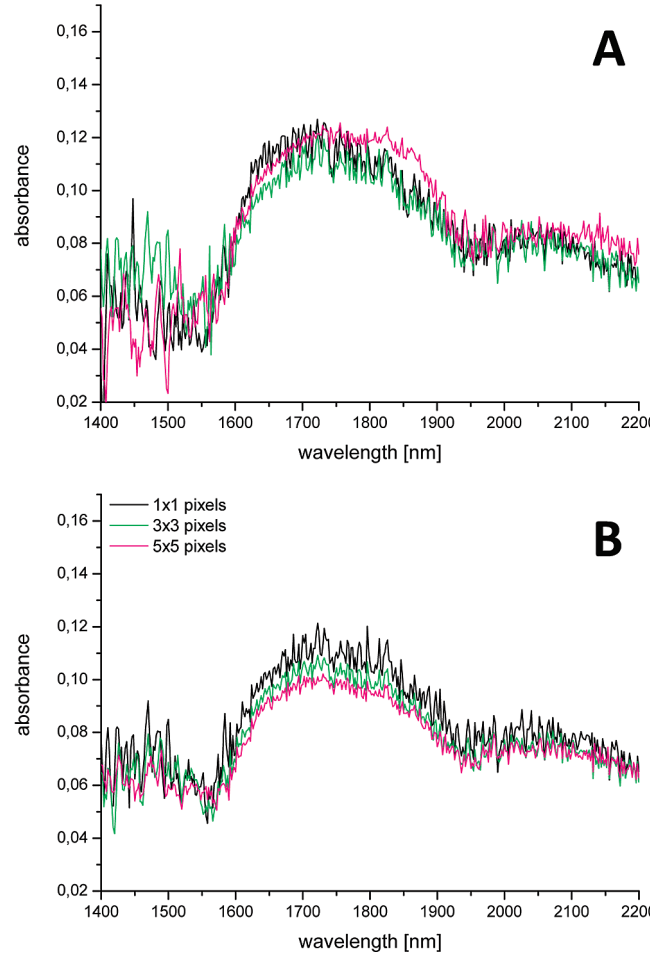

Figure 6. Absorption spectra of a single gold nanoshell in D_2O, calculated (A) from a single pixel at three different positions within the nanoshell and (B) calculated using data from a single pixel (black), an average of a square of 3 × 3 (green) and 5 × 5 (pink) pixel at the same position.

such as those in this study. When the LSPR bands are narrow, shifts in λ_{max} can be easily and accurately determined. However, as illustrated in Figures 6 and 7, the absorbance bands of our gold nanoshells are relatively broad. For example, values of the full width at half-maximum (fwhm) of the LSPR bands of the particles in formamide are as large as 300 nm. Such wide shifts of the plasmon bands are difficult to predict accurately. As a consequence, it has been proposed that for broad LSPR bands, it is more appropriate to consider a ratio of λ_{max} and fwhm (i.e., λ_{max}/fwhm) rather than the λ_{max} value alone.[31,32]

Correspondingly, Figure 9 shows plots of $(\lambda_{max}/\text{fwhm})^2$ for single gold nanoshells as a function of $2n^2$ (or 2ϵ) in six different solvents. A linear relationship was found for only three solvents: D_2O, acetonitrile-d_3, and ethyl acetate. Acetone-d_6 shows a slight deviation, whereas formamide and pyridine-d_5 exhibit distinctly different correlations. Specifically, formamide and pyridine-d_5 have $2n^2$ values of 4.21 and 4.56, respectively, which are much higher than those of D_2O, acetonitrile, acetone, and ethyl acetate, but their $(\lambda_{max}/\text{fwhm})^2$ values are considerably lower than those of these four solvents. At present, we have no clear

(29) Mulvaney, P. *Langmuir* **1996**, *12*, 788–800.
(30) Shosh, K. S.; Nath, S.; Kundu, S.; Esumi, K.; Pal, T. *J. Phys. Chem. B* **2004**, *108*, 13963–13971.
(31) Miller, M. M.; Lazarides, A. A. *Abstract of Papers, 231st ACS National Meeting*, Atlanta, GA, 2006.
(32) Miller, M. M.; Lazarides, A. A. *J. Phys. Chem. B* **2005**, *109*, 21556–21565.

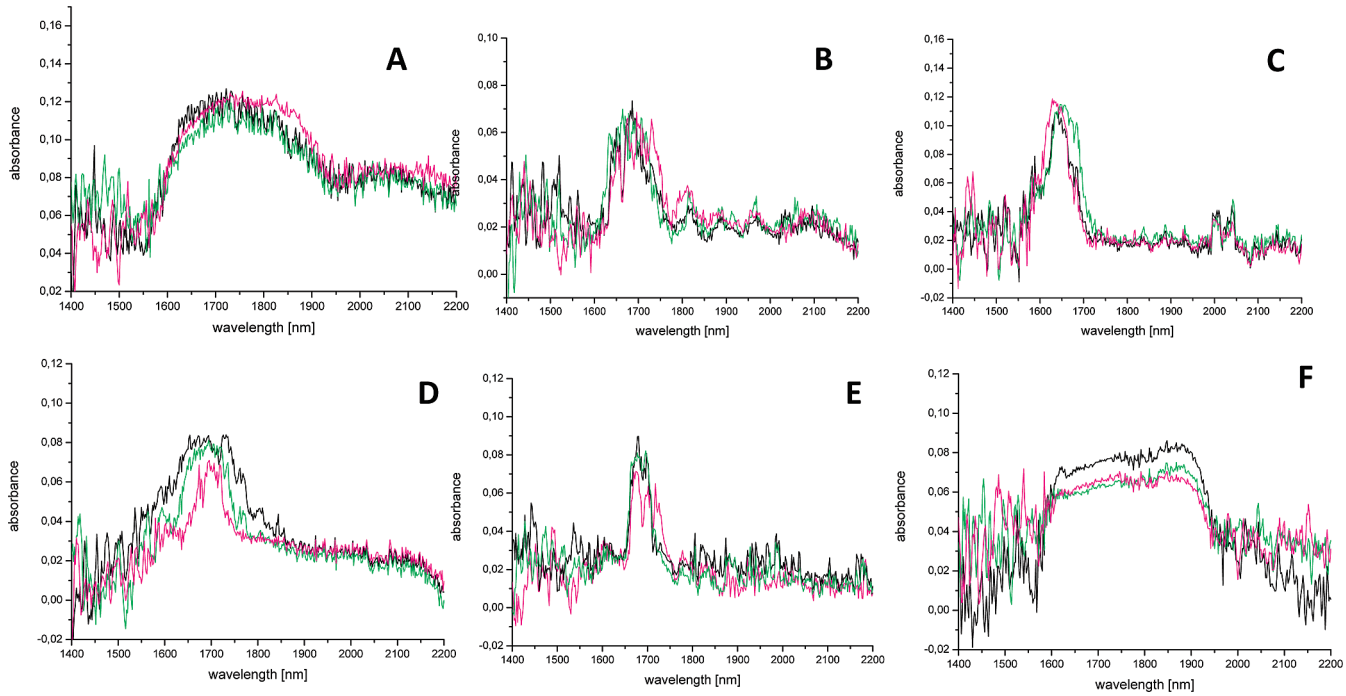

Figure 7. Absorption spectra at three different positions within the same single gold nanoshell in different solvents: (A) D_2O; (B) acetonitrile-d_3; (C) ethyl acetate; (D) pyridine-d_5; (E) acetone-d_6; and (F) formamide.

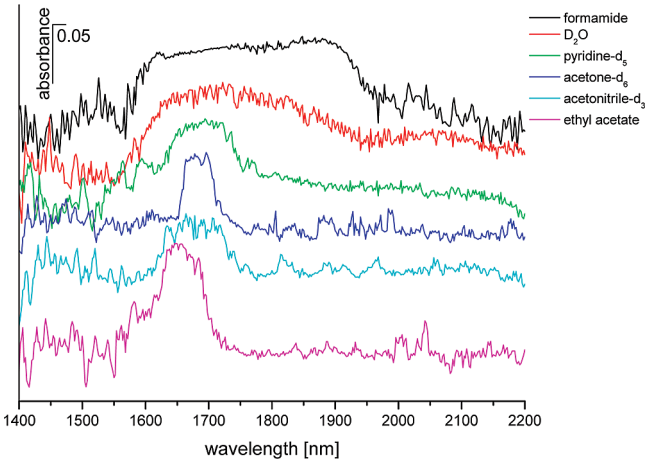

Figure 8. Absorption spectra of a single gold nanoshell in different solvents. Black: formamide; red: D_2O; green: pyridine-d_5; blue: acetone-d_6; neon green: acetonitrile-$d_3$and pink: ethyl acetate. For clarity the spectra were shifted vertically.

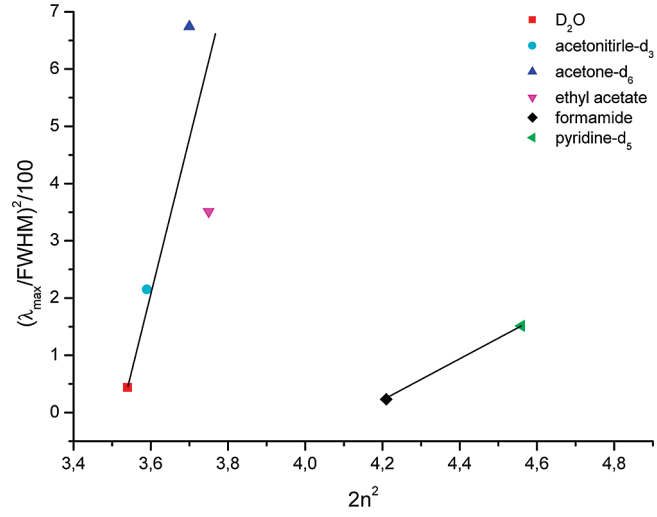

Figure 9. Plot of the square of the ratio of absorption maximum to full-width at half-maximum as a function of $2n^2$. Red square: D_2O; neon green circle: acetonitrile-d_3; blue triangle: acetone-d_6; pink triangle: ethyl acetate; black diamond: formamide; and green triangle: pyridine-d_5.

rationalization for this deviation, but it is probably due to the nature of the solvents and their capacity to interact with and perhaps bind to the surface of the nanoshell. This effect obscures the expected correlation between the refractive index of the solvent and the features of the LSPR bands. However, it is noteworthy to add that the non-linearity seen here is not new as it has been previously observed by many groups for LSPR characterization of particles in response to solvent as well as in adsorbates.[33−36]

In summary, we have successfully demonstrated for the first time that the NIR-MSI microscope can be successfully used to observe and measure *directly* the LSPR spectra of *individual* gold nanoshells. By directly measuring surface plasmon spectra of individual nanoshells, any features in the LSPR spectra that arise from the polydispersity of the nanoshells, or from variations in their aspect ratio, shape, and/or volume can be understood and interpreted. As expected, the LSPR of individual nanoshells measured by the NIR-MSI microscope agree well with the spectra calculated theoretically using Mie scattering for the nanoshells in this study (i.e., nanoshells with silica cores ~800 nm in diameter and gold shell thicknesses of ~35 nm).[24,25] Additionally, the NIR-MSI microscope also enables measurement of LSPR at different

(33) Thomas, K. G.; Zajicek, J.; Kamat, P. V. *Langmuir* **2002**, *18*, 3722–3727.
(34) Ghosh, S. K.; Nath, S.; Kundu, S.; Esumi, K.; Pal, T. *J. Phys. Chem. B* **2004**, *108*, 13963–13971.
(35) Ghosh, S. K.; Nath, S.; Kundu, S.; Esumi, K.; Pal, T. *Appl. Spectrosc.* **2005**, *59*, 844–847.
(36) Sanghamitra, N. J. M.; Mazumdar, S. *Langmuir* **2008**, *24*, 3439–3445.

positions within a single nanoshell. This feature can be effectively used to characterize and to gain insight into the properties of the nanoshells. For example, we found that the LSPR spectra are distinct at various positions within a single nanoshell. Since LSPR spectra are known to depend on the shape and morphology of the nanoshells, these observations seem to suggest that the nanoshells are not smooth and well-defined spheres as indicated on the scale of the SEM technique, but are rather rough and inhomogeneous (i.e., the shape and morphology vary within a single nanoshell).

Finally, the LSPR spectra of single nanoshells were found to depend on the dielectric constant of the medium. However, the relationship was determined to be more complex than simply following the Drude equation. Specifically, when $(\lambda_{max}/\text{fwhm})^2$ values of LSPR for single gold nanoshells were plotted as a function of $2n^2$ (or 2ϵ) for nanoshells in six different solvents, it was found that only three solvents exhibited a linear relationship: D_2O, acetonitrile-d_3, and ethyl acetate. Acetone-d_6 showed a slight deviation, whereas formamide and pyridine-d_5 exhibited distinctly different correlations. At present, we have no clear rationalization for this deviation, but it is possibly linked to the nature of the solvents and their capacity to interact with and perhaps bind to the surface of the nanoshells. This effect obscures the expected correlation between the refractive index of the solvent and the features of the LSPR bands. Experiments are now in progress to determine the origin of this deviation, and to use the NIR-MSI microscope to characterize other types of nanoparticles, including nanorods and nanocages.

ACKNOWLEDGMENT

The National Science Foundation (ECS-0404308), the Texas Center for Superconductivity, and the Robert A. Welch Foundation (Grant E-1320) provided generous support for the work at the University of Houston.

Received for review April 7, 2009. Accepted July 3, 2009.

AC9007495